Appendix C

CHAPTER-SPECIFIC NOTES

C.1. Notes for Chapter 2

Ru-P450 luminescence: dependence on concentration

Normalized luminescence decays at four concentrations (2, 4, 8, 12 μM) are superimposable.

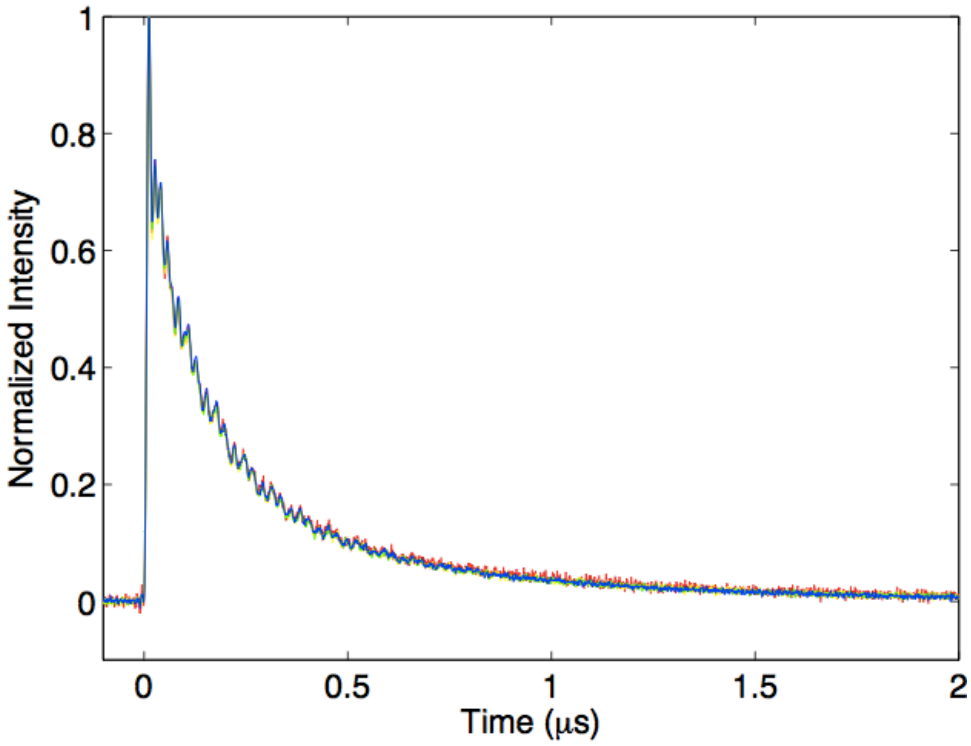

Figure C.1. Luminescence decays of Ru_{K97C}-BM3 at four concentrations. Red: 2 μM; Yellow: 4 μM; Green: 8 μM; Blue: 12 μM.

Low-temperature experiments

We have examined flash-quench of Ru-P450 BM3 at reduced temperatures to try and increase the lifetime of the observed compound II species. Solutions containing 25% glycerol enable examination of temperatures down to –15 °C. Luminescence lifetimes increase as temperature decreases, for both quenched and unquenched samples (**Figure C.2**). While it does appear that transient absorption features decay more slowly at low temperature, the magnitude of transient features

(and thus, yield of oxidized species) also decreases (**Figure C.3**). This strategy is unlikely to facilitate further characterization of photogenerated compound II.

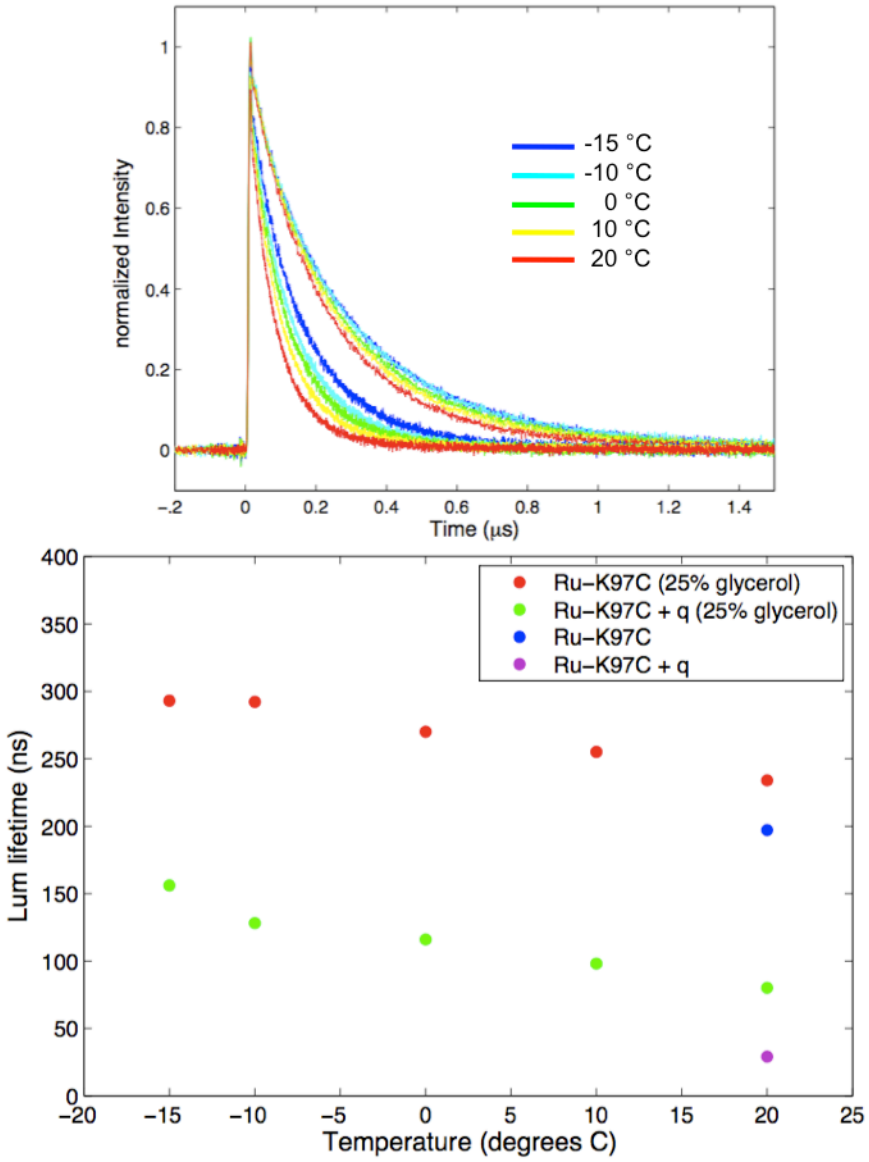

Figure C.2. Luminescence decays at variable temperature. **Top**: Quenched and unquenched luminescence decays of Ru_{C97}-BM3(W) at variable temperature. **Bottom**: Luminescence lifetimes at variable temperature.

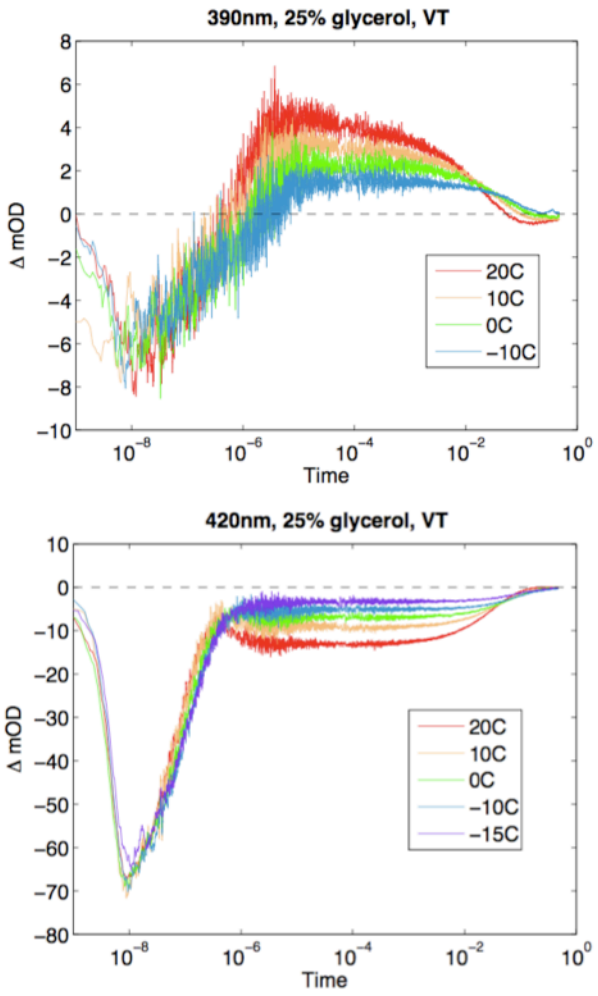

Figure C.3. TA at variable temperature for Ru_{K97C}-P450 BM3(W), pH 6.

C.2. Notes for Chapter 3

Search for the tryptophan radical cation intermediate

Tryptophan radical cation ($W^{\bullet+}$) and neutral radical ($W^{\bullet}$) species absorb in the visible region, with approximate extinction coefficients of $\varepsilon(\lambda_{max}$: 560 nm) = 3000 M^{-1} cm^{-1} and $\varepsilon(\lambda_{max}$: 510 nm) = 2300 M^{-1} cm^{-1}, respectively.[1] If such a radical species is indeed formed as a true intermediate along the multi-step electron transfer pathway, it is theoretically possible that we could observe it by transient absorption. Using the Ru_{K97C}-$P450_{BM3}$(W96) system (in which we have observed

photochemical heme oxidation) we have examined TA of the 500-600 nm region to see if such an intermediate can be identified.

We first examined flash-quench of the photosensitizer model complex $[Ru(bpy)_2(Aphen)]^{2+}$ to determine absorption components of the photosensitizer in this region. Approximate transient difference spectra at various timepoints were generated using ΔOD from single-wavelength data. We the examined Ru_{K97C}-$P450_{BM3}(W_{96})$ and Ru_{D77C}-$P450_{CYP119}({}_{H}W_{76})$, and generated analogous transient difference spectra.

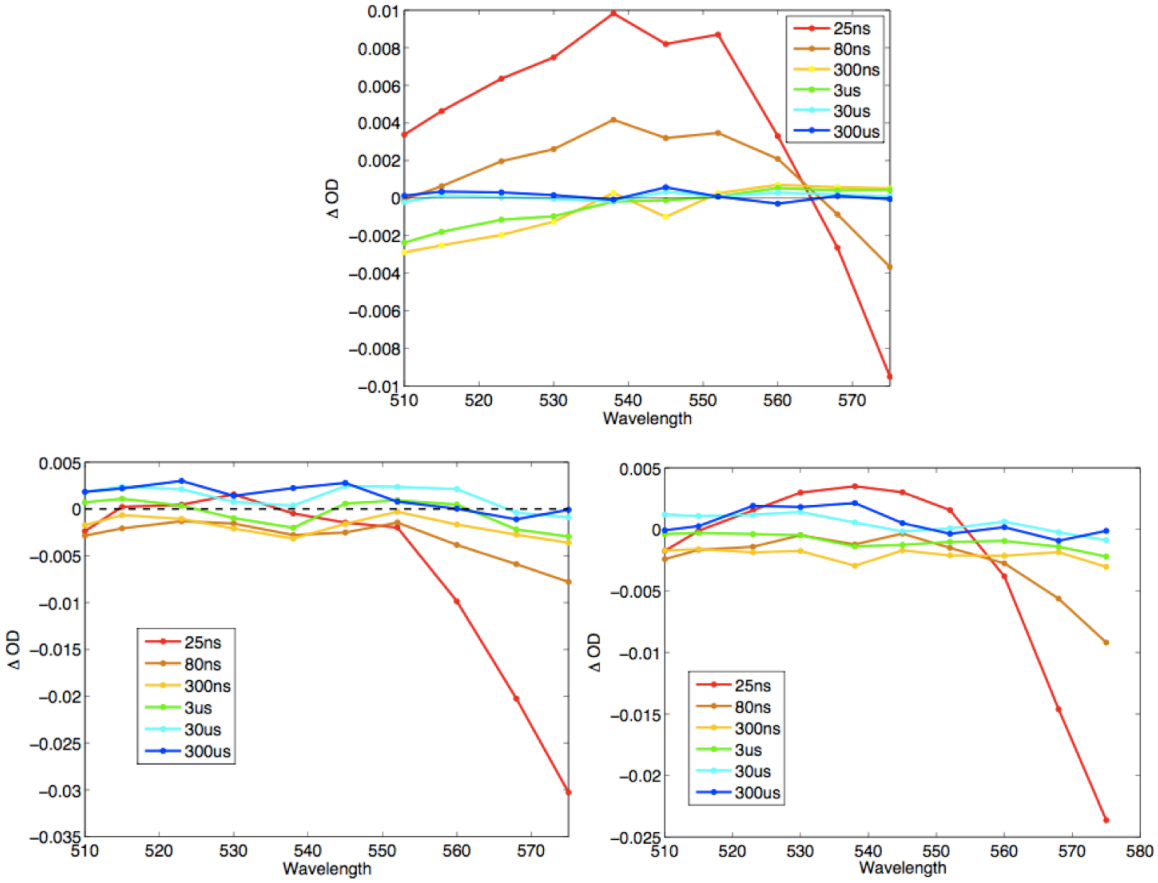

Figure C.4. Transient difference spectra of $[Ru(bpy)_2(Aphen)]^{2+}$ (top), Ru_{K97C}-$P450_{BM3}$(W96) (bottom left) and Ru_{D77C}-$P450_{CYP119}$(H76W) (bottom right) at various time points following excitation at 480 nm and quenching with $[Ru(NH_3)_6]^{3+}$.

As seen for $[Ru(bpy)_2(Aphen)]^{2+}$, the ruthenium excited state ($*Ru^{II}$) absorbs in the 500-570 nm region. Photons from excited state emission give rise to the apparent bleach from 560-580 nm. The Ru^{III} species is characterized by a bleach of the MLCT band, which tails into the 510-540 nm region; this species can be seen at 300 ns and 30 μs timescales. There is no increase at 510 nm or 560 nm associated with the oxidized photosensitizer.

If we are to identify any tryptophan radical species as true intermediates in the electron transfer pathway, we must observe their formation prior to that of heme oxidation (i.e., porphyrin radical cation formation); this occurs within 10 μs. Unfortunately, we are unable to detect any increases in absorbance on this timescale for the W-containing Ru-P450 conjugates. Additionally, TA on longer timescales are complicated by the P450 Q-bands; these also absorb in the 500-600 nm with extinction coefficients > 10,000 $M^{-1}cm^{-1}$, and are expected to shift upon oxidation of the heme. It is quite likely that heme-associated TA signals will obscure any possibility of observing the tryptophan radical.

C.3. Notes for Chapter 5

Selection of probe wavelength for CO rebinding kinetics

For single-wavelength transient absorption measurements, it was observed that the arc-lamp probe light was enough to induce CO-photolysis and generate the inactive form: P420. Thus, a narrow bandpass filter (centered at 406 nm, **Figure C.5**) was used to reject the majority of the probe light. This wavelength has large ΔOD associated with the interconversion between Fe^{II} and Fe^{II}-CO forms, and is far enough from the Soret peak that it causes little photolysis.

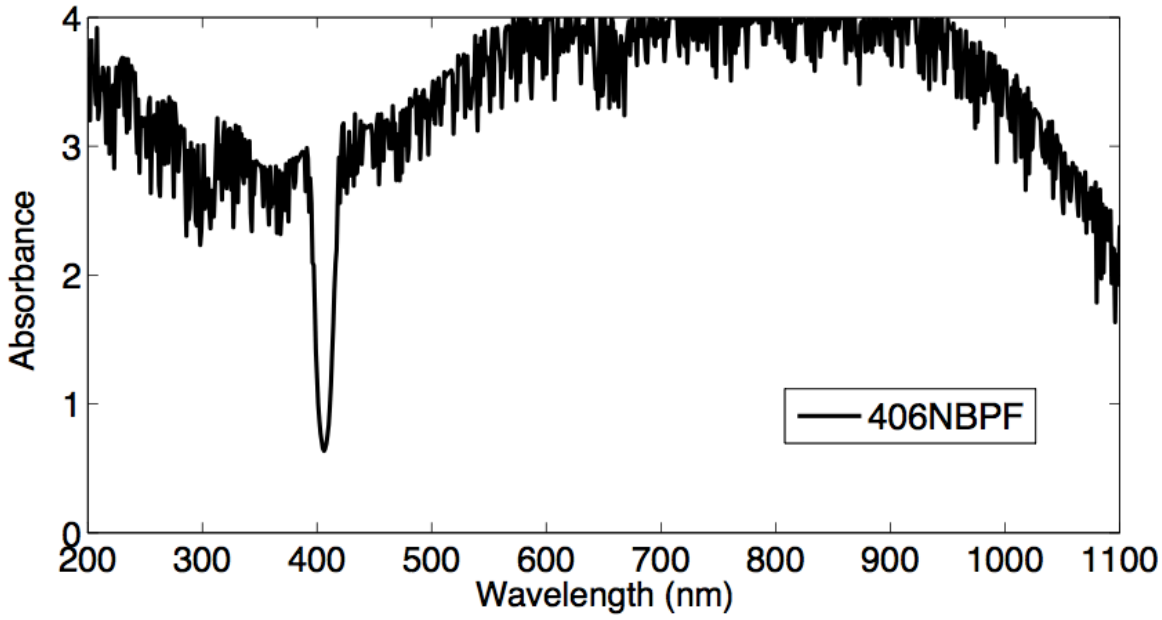

Figure C.5. 406 nm narrow band pass filter.

Overlay of PSI and NSI kinetics traces

Single-wavelength transient absorption data collected on the picosecond-to-nanosecond timescale ("PSI") and the nanosecond-to-second timescale ("NSI") overlay well when multiplicatively scaled. PSI data are significantly noisier, with potential variation in laser power or sample integrity over the course of the measurement; therefore, we have scaled PSI data to match the NSI data (**Figure C.6**). Signal averages for each timescale were: 5 ns (10,000); 50 ns (10,000); 2 μs (150); 2 μs (150); 100 μs (150); 10 ms (5).

It is important to note that the scaled signal magnitude at time-zero (**Figure C.6,** magnitude of the red trace) is significantly larger than the maximum signal magnitude expected for this sample (~370 mOD vs. 270 mOD). Signal at very early timepoints (< 1 ns) may correspond to an excited state, associated with different absorptivities than the free Fe^{II}-CO. Until this magnitude discrepancy is resolved, it is not reliable to take the initial signal magnitude as the photolysis yield.

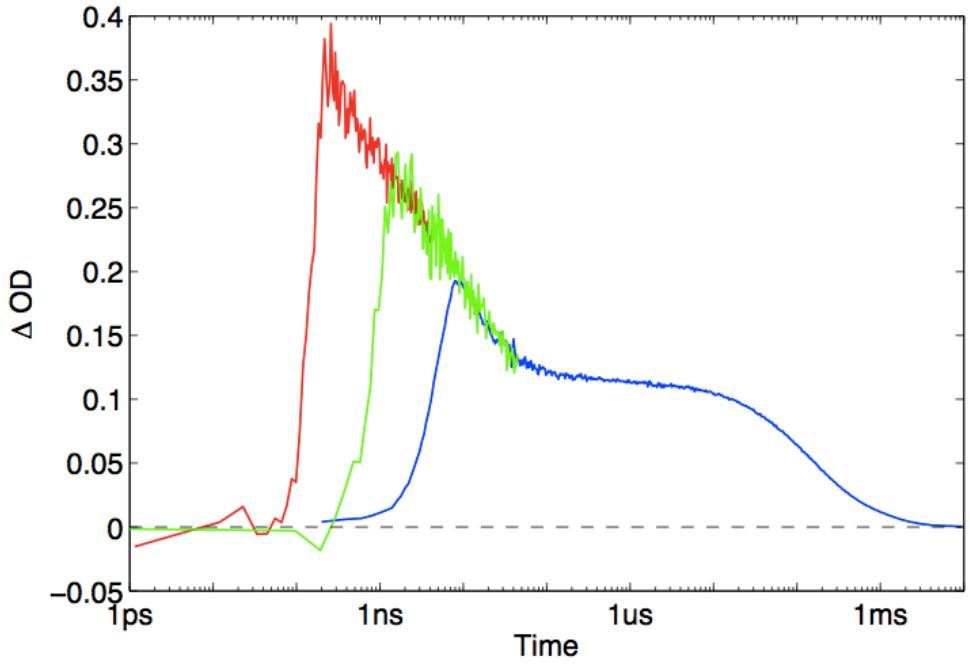

Figure C.6. Overlay of PSI and NSI data for CO rebinding kinetics in CYP119. PSI data (5 ns: red; 50 ns: green) is scaled by ~0.5 to overlay with NSI data (2 μs – 10 ms: blue).

Nonlinear least squares fitting of CO rebinding kinetics at various temperatures

We have subjected picosecond-to-millisecond TA data (collected at temperatures 10-70 °C) to a non-negative least squares fitting method (**Figure C.7,** see Appendix D for sample matlab script). The positive amplitudes at rate constants ($\log_{10}(k)$) greater than 10 are faster than the instrument response; these are an artifact of the fitting procedure, and have been ignored in the remainder of our analysis.

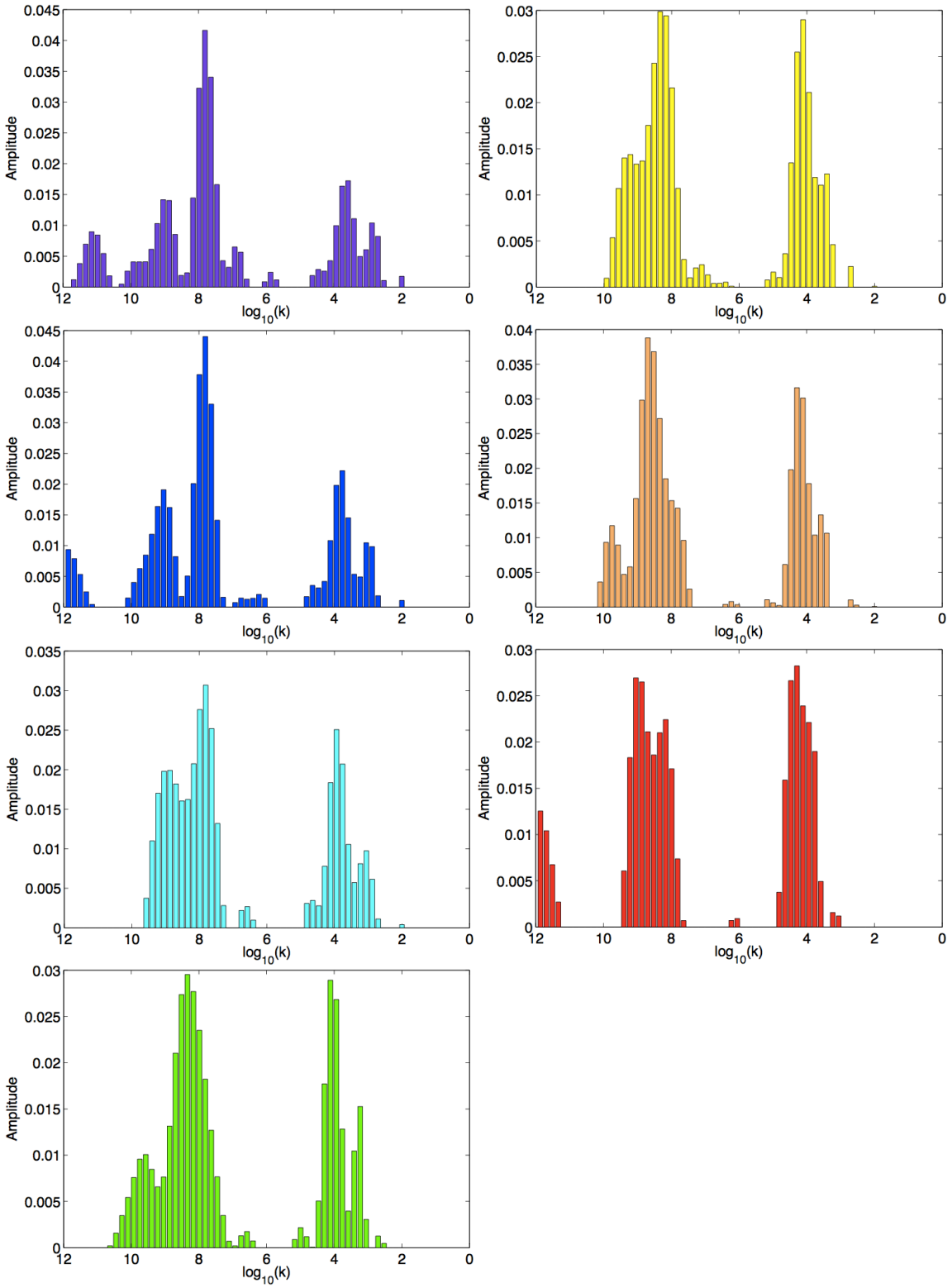

Figure C.7. Rate constant amplitudes from nnls fitting of CO rebinding ps-to-ms TA data at various temperatures. Purple: 10 °C; Blue: 20 °C; Cyan: 30 °C; Green: 40 °C; Yellow: 50 °C; Orange: 60 °C; Red: 70 °C.

C.4. Notes for Chapter 6

Determination of ferrous/ferric ratio

We have used a Matlab script (appendix D) to determine the ferrous/ferric ratio in each intermediate spectrum during potentiometric titration. An example is shown below: all ferrous is cyan, all ferric is green, the experimental data is blue, and the model, using 70% of the ferrous component, and 30% of the ferric component, is shown in red dashes.

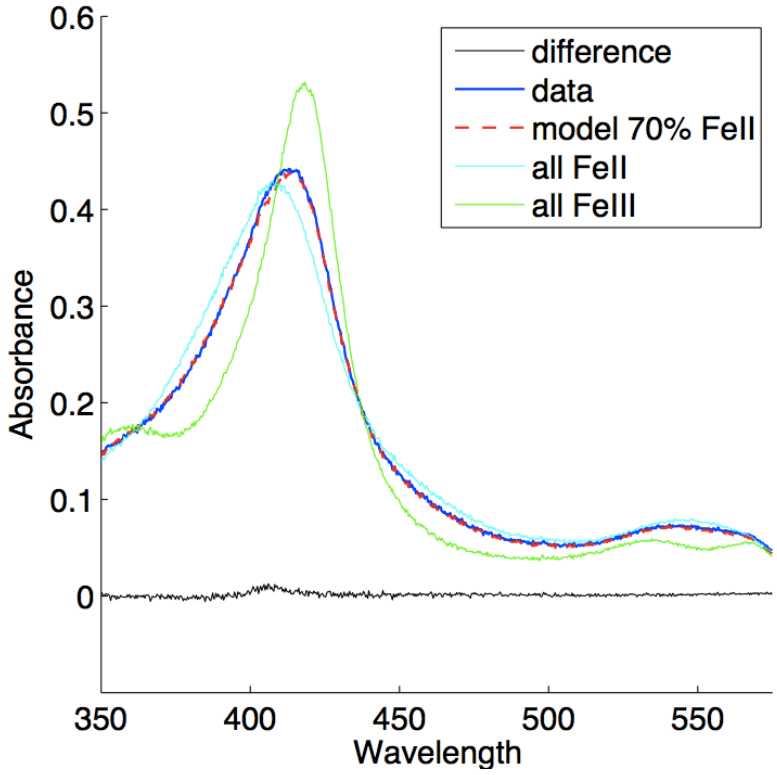

Figure C.8. Decomposition of a spectrum into ferric and ferrous components using the script: spectraldeconvoluter.m.

Reproducibility

The figure below shows potentiometric titrations for two batches of wild type P450 BM3. The two protein samples were expressed and purified in separate labs (dark

green: Arnold group; light green: Gray group), measurements were performed 3 months apart, using different electrodes (dark green: Pt mesh working, Pt wire counter, Ag/AgCl reference with vycor frit; light green: Au wire working, Pt wire counter, Ag/AgCl reference with salt bridge). The resulting potentials are within 20 mV of one another.

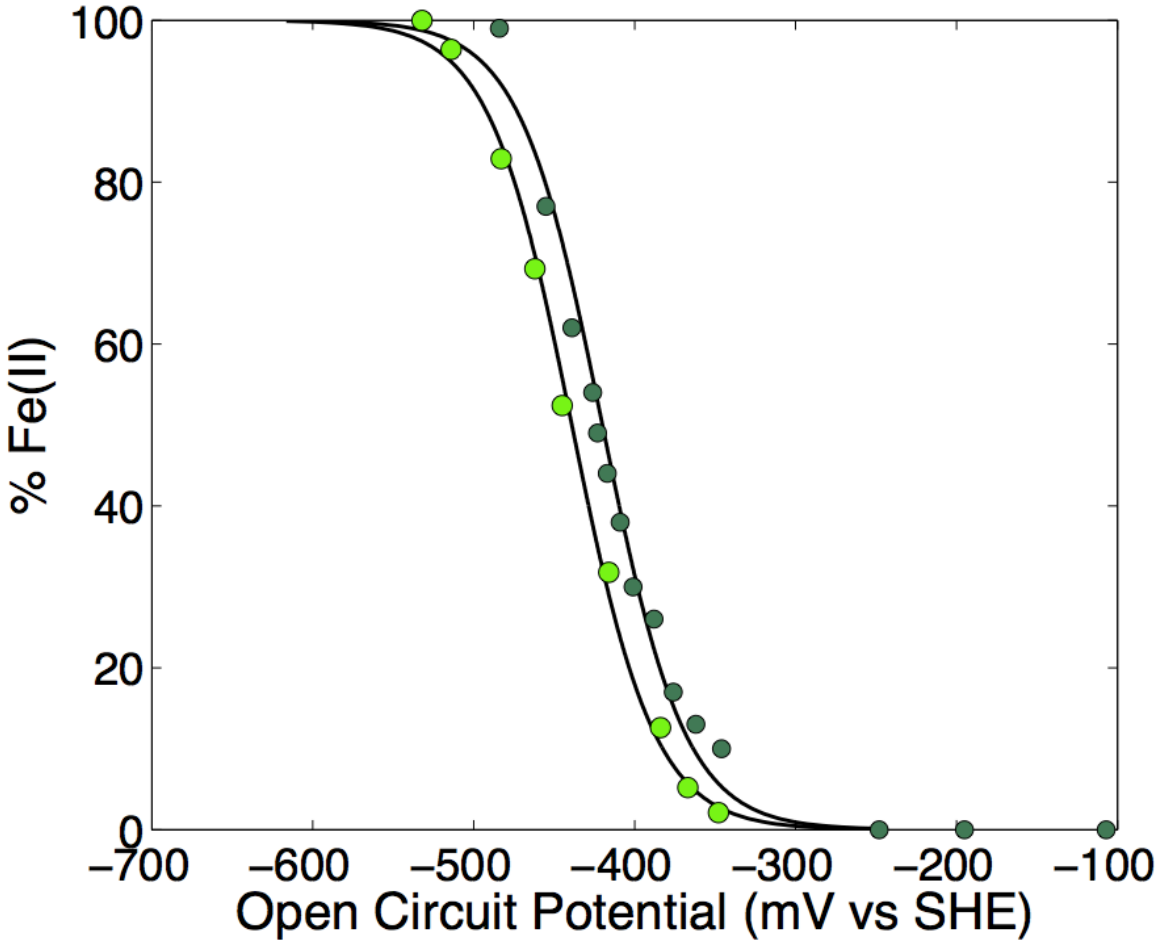

Figure C.9. Two separate potentiometric titrations of wild type P450 BM3.